CWE-8
June 7-11, 2026
London, ON, Canada

A benchmark of the aerodynamics of a medium-rise building tested in different wind tunnels and conditions

Stefano Brusco[a], Timothy J. Acosta[a], Yitian Guo[a], Jin Wang[a], Jon Galsworthy[b], John Kilpatrick[c], Gregory A. Kopp[a]

[a]*Faculty of Engineering, London, Ontario, Canada, sbrusco@uwo.ca*
[b]*CPP Inc., 7365 Greendale Rd, Windsor, CO, 80550, USA*
[c]*RWDI, 600 Southgate Drive, Guelph, Ontario, Canada*

SUMMARY

This objective of this paper is to present a benchmark dataset and analysis of the aerodynamics of a gable-roofed medium-rise building tested at RWDI, CPP, and Western University by means of independent wind tunnel test campaigns. Using 1:100 wind-tunnel models instrumented with pressure taps, five atmospheric boundary layer exposures were reproduced to capture mean and fluctuating pressures under well-defined inflow conditions. The database provides repeatable measurements suitable for validating CFD simulations of bluff-body flows. Results across exposures with similar wind-field characteristics show consistent global loading, while differences in turbulence intensity and structure significantly influence pressure distributions. These effects vary with building orientation, reflecting changes in separation, reattachment, and vortex behaviour, key features that CFD models often struggle to reproduce. Overall, the dataset offers a controlled, high-quality reference for assessing turbulence-model performance and improving CFD predictions of wind-induced loads on low-rise structures.

Keywords: *wind tunnel test, medium-rise building, benchmark of aerodynamics.*

1. INTRODUCTION

To support the ASCE 7 (American Society of Civil Engineering) Main Wind-Force Resisting System (MWFRS) Consolidation Project (Guo et al., 2025), the project team at Western University (Western) performed a series of wind tunnel tests to investigate the wind effects on buildings with sloped roofs. Specifically, the aerodynamic database that was developed in such study consists of 156 different configurations (74 gable and 82 hip roof-shaped building cases, all with a roof slope of 6/12). The turbulent Atmospheric Boundary Layer flows that were generated were calibrated to simulate both “Open” and “Suburban” terrain categories.

As a benchmark study, one of the geometries of the gable roof-shaped building cases (for a ~3:1 rectangular cross-section) was also tested by Rowan Williams Davies and Irwin (RWDI), Inc., and Cermak Peterka Petersen (CPP), Inc., for comparable wind field exposures. This abstract examines the results gathered from the different databases. Firstly, the different vertical profiles of mean wind velocity and turbulent properties of the wind field are discerned. Based on them, meaningful comparison in terms of mean, fluctuating and peak loads are conducted, verifying the consistency of the results taking the measurement uncertainties into account. Secondly, the effects played by the different turbulent properties of the tested exposures on the aerodynamics of the wind tunnel model are assessed.

2. DESCRIPTION OF THE BENCHMARK DATASET

The geometry of the commonly tested structure is indicated in Figure 1. It is characterized by a plan width, *w*, equal to 12.19 m, and by the other plan dimension, *d*, equal to 38.10 m. The

eave height of the gable roof, h_e, is 48 m, and the total heigh, h, is 51.05 m.

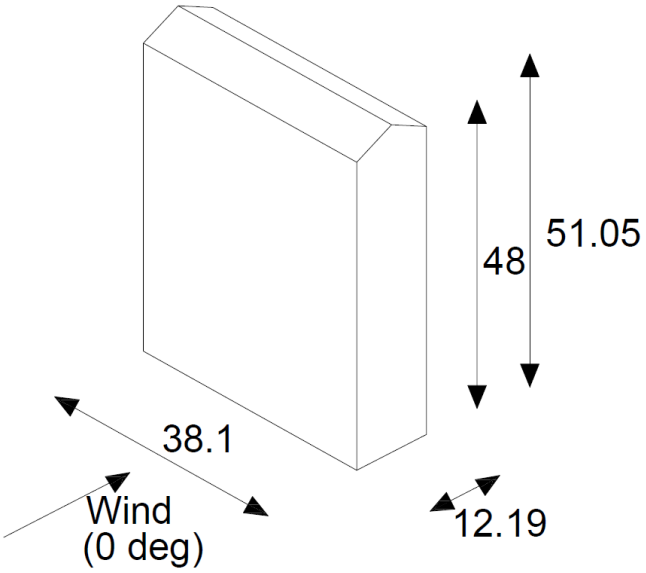

Figure 1: Geometry of the benchmark gable-roofed building (full-scale dimensions, in meters).

All three laboratories tested 1:100 scale replicas of the same gable-roof geometry, each equipped with a dense, nearly uniform array of pressure taps over all exterior surfaces. The models were tested in isolation for wind directions from 0° (wind normal to the long face) to 90° (wind normal to the short face) in 10° increments. Table 1 summarizes key characteristics of the testing campaigns performed at the three facilities. The third column reports the turbulence intensity I_u, expressed as a percentage and defined as the ratio of the standard deviation of the longitudinal velocity fluctuations to the corresponding mean value.

Table 1: General overview of the wind tunnel test campaigns performed by RWDI, CPP and Western

Label	Number of tested wind exposures	I_u (%) at h	Number of pressure taps	Sampling frequency (Hz)
RWDI	1 (Open)	15	632	512
CPP	2 (Open, Suburban)	15, 22	796	250
Western	2 (Open, Suburban)	12, 20	800	625

The comparison of wind loading begins with global response metrics, including base shear and overturning and torsional moments. It is important to note that the differences in total tap counts reported in Table 1 arise primarily from variations in the roof tapping layouts. In contrast, the wall surfaces share a consistent tap arrangement across all laboratories. Consequently, comparisons of wall pressure distributions along corresponding tap lines provide a reliable basis for assessing dataset consistency and serve as meaningful reference cases for CFD validation.

3. PRELIMINARY RESULTS AND CONCLUSIONS

The comparisons are conducted in two steps. Firstly, tests characterized by similar wind fields are considered (i.e., “Open” or “Suburban” exposures only, Table 1). The results in terms of

mean load coefficients are excellent and within measurement uncertainties, as well as those concerning fluctuating loads. Besides, the comparison in terms of peak coefficients lets transpire a satisfactory agreement. When comparing the results coming from the 5 different datasets (second step), the role played by the different exposures stands out. In particular, the different mean wind field seems to influence the mean aerodynamic loading, while the different turbulent properties are reflected on the fluctuating load coefficients. Moreover, the effects played by the turbulence appear to be different with the considered wind direction. For the purpose of this abstract, focus will be given to 0 and 90 degrees of incidence. These conditions constitute two significantly different situations for the building from an aerodynamic perspective (e.g., Yu et al., 2012). In fact, for 0 degrees (Figure 1), the shear layers separated from the leading edge of the structure do not reattach on its lateral sides. Conversely, the flow reattachment occurs for 90 degrees and for the considered levels of turbulence intensity. These facts may have a repercussion on the applicability of the quasi-steady theory (e.g., Holmes, 2015) to predict the peak loading.

To facilitate the comparison between the different datasets, a ring of pressure taps of the cross-section of the building is analyzed. This is located at 32.6 cm (~0.7 h_e) from the ground, and it is composed of 32 pressure sensors. The nominal position of each of them is the same for all the datasets. The mean and fluctuating pressure distributions are employed to estimate the time-varying drag and the lift coefficients of the cross-section with the wind direction. These values may be compared to data from various literature, although mostly related to two-dimensional configurations. For the wind oriented at 0 degrees, the aerodynamic of the cross-section is compared to the data provided by Bearman and Trueman (1972), Norberg (1993) and Yang and Mason (2019) for 1/3 side ratio (large side perpendicular to the wind direction). On the other hand, for 90 degrees of wind orientation, the data are compared with Norberg (2003), Noda and Nakayama (2003) and Yang and Mason (2019) for 3/1 side ratio.

Concerning that ring of pressure taps and the 90 degrees wind orientation, Figure 2 shows the variation of the mean (Figure 2a), $\bar{C}_p$, and the standard deviation (Figure 2b), σ_{Cp}, of the relevant pressure coefficients, C_p, which is defined as:

$$C_{p_{ref}} = \frac{P - P_o}{\frac{1}{2}\rho \bar{u}_h^2}, \tag{1}$$

where P is the measured pressure, P_o is the static pressure, ρ is the air density, $\bar{u}_h$ is the mean wind velocity at the mean roof height. The abscissa indicates the non-dimensional perimeter of the cross-section, which is made non-dimensional by dividing it with the side dimension d. The dashed vertical lines indicate the separation between windward (on the right side), leeward (the second one from the left) and lateral sides.

Observing the data in Figure 2, the role played by the different properties of the considered wind fields is already qualitatively graspable.

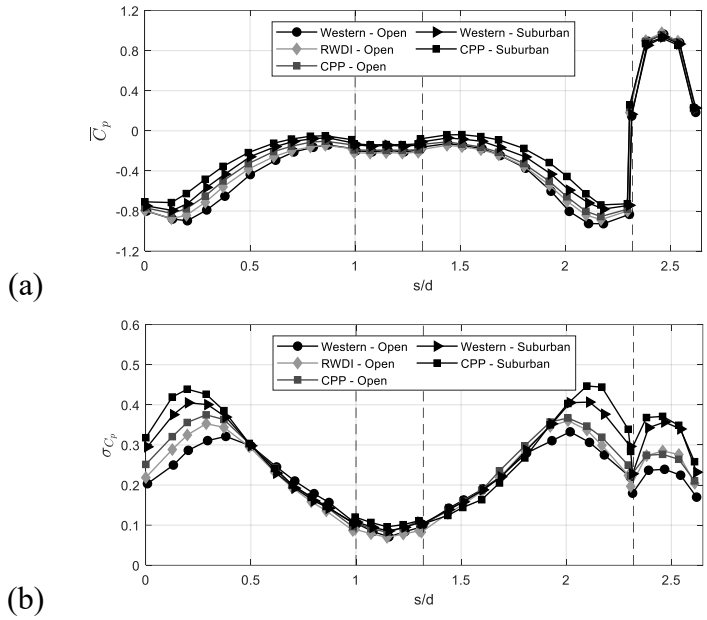

Figure 2. Mean (a) and standard deviation (b) of the pressure coefficients for wind oriented at 90 degrees on the analyzed ring extracted from the five different datasets.

In particular, the mean pressure distribution shows stronger suction in the afterbody region under "Open" exposures, whereas higher turbulence levels in "Suburban" flows lead to increased mean pressure coefficients. The standard deviation of the pressure coefficients likewise increases when transitioning from "Open" to "Suburban" conditions. The turbulence intensity also affects the location of the peak standard deviation, suggesting shifts in the dominant vorticity patterns around the building.

The full paper will quantify these differences in detail and will incorporate measurement uncertainty into the analysis. From a CFD perspective, the observed sensitivity to inflow turbulence, flow reattachment behaviour, and vorticity distribution underscores the importance of accurately prescribing boundary-layer conditions and turbulence characteristics in numerical models. The dataset therefore provides a valuable benchmark for assessing the ability of RANS, LES, and hybrid approaches to capture these aerodynamic mechanisms.

REFERENCES

Bearman, P.W., Trueman, D.M., 1972. An investigation of the flow around rectangular cylinders. Aeronautical Quarterly 23, 229-237.

Guo, Y., Wang, J., Acosta, T.J., Brusco, S., Kopp, G.A., 2025. Methodology for obtaining aerodynamic coefficients for unified wind loading provisions. Journal of Structural Engineering 151 (11), 04025182.

Holmes, J.D. 2015. Wind Loading of Structures, CRC Press, Boca Raton, FL, USA.

Noda, H., Nakayama, A., 2003. Free-stream turbulence effects on the instantaneous pressure and forces on cylinders of rectangular cross-section. Experiments in Fluids 34, 332 – 344.

Norberg, C., 1993. Flow around rectangular cylinders: pressure forces and wake frequencies. Journal of Wind Engineering and Industrial Aerodynamics 49, 187–196.

Yang, T., Mason, M.S., 2019. Aerodynamic characteristics of rectangular cylinders in steady and accelerating wind flow. Journal of Fluids and Structures 90, 246–262.

Yu, D., Butler, K., Kareem, A., Glimm, J., Sun, J., 2013. Simulation of the Influence of Aspect Ratio on the Aerodynamics of Rectangular Prisms. Journal of Engineering Mechanics 139 (4), 429 - 438.